

Calculations of Neutron and Proton Induced Cross Sections on Tungsten up to 3 GeV

Hirohiko KITSUKI, Satoshi Kunieda, Nobuhiro SHIGYO, Kenji ISHIBASHI
Department of Applied Quantum Physics and Nuclear Engineering, Kyushu University
Hakozaki, Higashi-ku, Fukuoka 812-8185
e-mail:kituki@meteor.nucl.kyushu-u.ac.jp

Neutron and proton-induced cross section on tungsten were calculated in the energy region from 20 MeV up to 3 GeV for nuclear data evaluation. Reparameterization of optical model potential for tungsten target is made by modification of reported global parameter set. Nucleon emission spectra from (p, xn) , (n, xn) , (p, xp) and (n, xp) reaction are evaluated by use of moving source model.

1 Introduction

Nuclear data covering incident energies up to several GeV are required for applications such as radiation transport simulations in the high-intensity neutron source and the accelerator-driven transmutation of nuclear wastes. For the design of target of spallation neutron source, especially, it is necessary to know the reaction rate and particle production of tungsten in the energy region up to several GeV accurately. In this study, neutron and proton induced cross sections of tungsten were calculated up to 3 GeV for nuclear data evaluation. Optical model parameters were determined for incident proton and neutron up to 250 MeV. New parameterization of optical model was obtained by adjusting the global optical potential parameter sets to the measured data for tungsten target. Activation yields for incident proton and neutron below 150 MeV at the energies below 150 MeV were calculated by GNASH code[1] with transmission coefficients derived from this optical model analysis. Ones at the energies below 3 GeV were computed by QMD+SDM (Quantum Molecular Dynamics + Statistical Decay Code) code[2]. The MS model[4] based on the Maxwell-like distribution was employed to analyze the nucleon emission double cross section in the incident proton energy region up to 3 GeV. In the forward direction of neutron emission, the Gaussian term was introduced into the MS model with momentum transfer-based parameterization[4]. The present work takes the experimental data on W target. Results of the QMD+SDM code are also used to give the cross sections in the neutron region where no measured data are available.

2 Description of calculation model

2.1 Optical model analysis

Global potential parameters for incident neutrons from 10 to 80 MeV are obtained by Walter and Guss[6]. In incident energy region from 50 to 400 MeV, proton and neutron global optical potentials are parameterized by Madland[7]. In this work, these optical potential was reparameterized to reproduce neutron and proton cross sections accurately.

The general potential form factor having Woods-Saxon form for V_r and W_v and Thomas-Fermi form for spin-orbit are used as

$$U(r) = - V_r f_v(r) - iW_v f_w(r) + 4ia_{wd}w_d \frac{df_{wd}(r)}{dr} - \frac{1}{r} \left(\frac{\hbar}{m_\pi c} \right)^2 \left(V_{so} \frac{d}{dr} f_{vso}(r) + iW_{so} \frac{d}{dr} f_{uso}(r) \right) \mathbf{l} \cdot \mathbf{s}, \quad (1)$$

where m_π is the mass of pion, and the form factors f standard Woods-Saxon shape. Incident energy dependency of parameters by Madland and by Walter and Guss are adjusted to the experimental data for W target. Potential parameters V_r and W_v are shown in Fig. 1 for neutron and proton incidence. Dashed lines and dotted lines stand for parameters by Madland and by Walter and Guss, respectively. The quantities reparameterized in this analysis are indicated by solid lines. Since experimental data for polarized particle incidence are poorly measured for W target in the incident energy region, parameters set of spin-orbit terms obtained by Walter and Guss and ones by Madland were applied for following calculations of cross sections.

2.2 Emission cross section

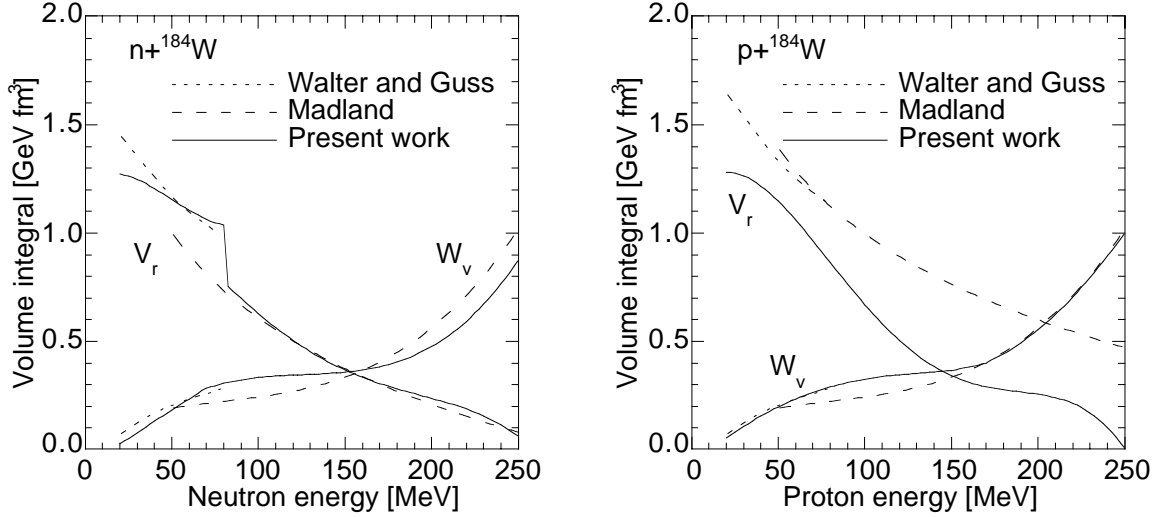


Figure 1: Volume integrals of V_r and W_v

Calculation of the light particle emission cross sections up to 200 MeV was performed by use of GNASH[1] based on the exciton model of Kalbach and Hauser-Feshbach statistical theory. Quick-GNASH code system[3] originating from GNASH was employed in this calculation. The transmission coefficients for neutron and protons calculated from the optical model analysis are utilized to GNASH calculation

The excitation of the giant isoscalar broad resonances(GR) was accounted for the calculation of neutron inelastic scattering, which is dominant for low-excited scattering induced by several-tens MeV nucleon[5]. In this analysis, deformation parameters effectively were determined by searching for the experimental angle integrated inelastic cross section[13] with utilization of PREGNASH code. Lorentzian shaped function was used to evaluate the contribution of giant resonance. The equation is written as

$$\left(\frac{d\sigma}{dE}\right)_{GR} = \sigma_{GR}\Gamma^2 / \left((E - E_{GR})^2 - \frac{\Gamma^2}{4}\right), \quad (2)$$

where σ_{GR} and E_{GR} are adjustable parameters, and are fitted to the results calculated by use of effective deformation parameter. The distribution width $\Gamma = 5$ MeV broadened by the fragmentation of the giant resonances in deformed nuclei was used[5].

For computing cross sections above 100 MeV, QMD+SDM code was used. In QMD+SDM code, dynamical process is calculated by QMD and the contribution derived from the statistical process is obtained by the SDM. The QMD codes takes a semiclassical simulation method in which each nucleon state is represented by a Gaussian wave function. The SDM code considers n , p , d , t , ${}^3\text{He}$ and α evaporation.

2.3 Nucleon production double differential cross sections

Calculations of nucleon production double differential cross sections were performed by the use of moving source(MS) model. In this model, nucleons are assumed to be emitted isotropically with an exponential-type energy distribution at a temperature T (MeV) in the moving frame. For the spallation reaction induced by nucleons about above a hundred MeV, the nucleon emission double differential cross section in the laboratory frame is expressed by a form of summation of three exponential-components as the cascade, the preequilibrium and the evaporation. In the forward emission direction below 30° , the quasi-elastic and -inelastic scattering processes are dominant in this region, and the neutron emission spectrum is strongly forward-peaked. In this work, simple Gaussian shaped term for evaluation of forward-peaked emission spectra is combined with three components of the MS model. Nucleon emission spectra is analyzed by the equation[4] as,

$$\left(\frac{d^2\sigma}{d\Omega dE_{kin}}\right)_{MS+G} = \sum_{i=1}^3 pA_i \exp\left\{-\left(\frac{E_{kin} + m - p\beta_i \cos\theta}{(1 - \beta_i^2)^{\frac{1}{2}}} - m\right)/T_i\right\}$$

$$+ A_G \exp \left\{ -\frac{(E_{kin} - E_G)^2}{\sigma_G^2} \right\}, \quad (3)$$

Three components of $i = 1$ to 3 of the first term in the right side of Eq. 3 correspond to individual processes of the cascade, the preequilibrium and the evaporation, respectively. In this term, E_{kin} and p is the kinetic energy (MeV) and the momentum (MeV/c) of an emitted neutron in the laboratory frame, respectively and m the neutron mass (MeV). Quantities A_i , β_i and T_i are called amplitude, velocity and temperature parameters, respectively. A_G , E_G and σ_G are quantities with dependency of incident particle momentum-transfer, and represents emission spectra originated from the quasi-elastic and quasi-inelastic-like scattering. The parameters are adjusted to the experimental nucleon emission spectra and the calculated data results by QMD+SDM. For the spallation reaction at incident nucleon energies up to 3 GeV, the fitting by Eq. 3 well reproduces the experimental data for wide target mass range of C to Pb[4].

3 Results and comparison

3.1 Total, elastic and reaction cross section

Total and Reaction cross section and elastic angular distribution were calculated by use of optical potential parameters obtained by this analysis. Figures 2, 3 and 4 show neutron total cross section, proton reaction cross section and neutron angular distribution of ^{184}W , respectively. The results by use of new optical parameters are represented by solid curves. For comparison, LA150 evaluations are indicated by dashed curves. Our optical parameters give good agreement with the experimental data[8][9][11][10][12] over wide incident energy range.

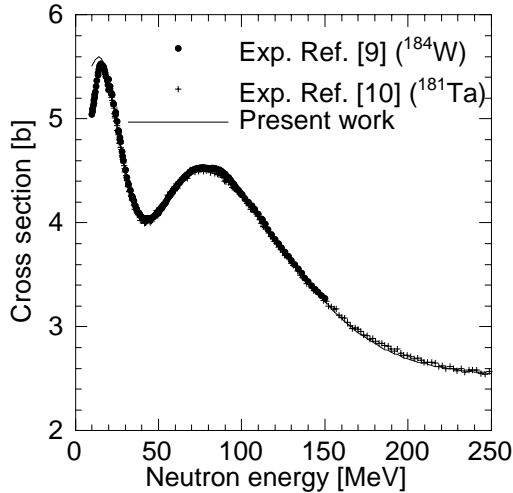


Figure 2: Neutron total cross section of ^{184}W

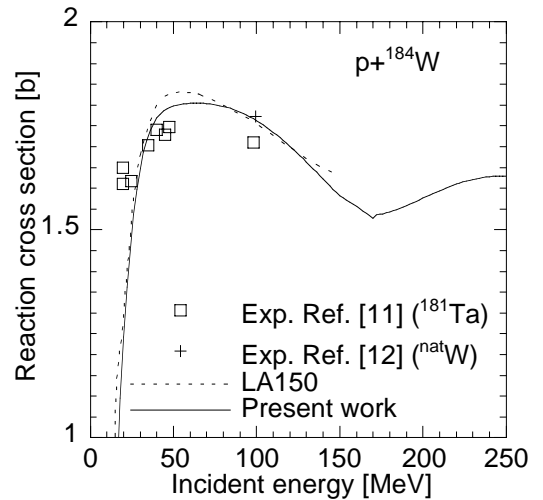


Figure 3: Proton reaction cross section of ^{184}W

3.2 Light particle emission

The (n, n') reaction cross sections for 26.5 MeV neutron incidence are shown in Fig. 5. Dashed curve indicates GNASH calculation, dotted one evaluation of giant resonance component by Eq. 2 with searching effective deformation parameters. Solid line stands for the sum of GNASH calculation and the component of giant resonance. The Lorentzian function adjusted for effective deformation parameters reproduce inelastic neutron emission about above 17 MeV well.

n , p , d , t , ^3He and α emission cross sections are shown in Fig. 6. Solid lines with marks stand for the results calculated by QMD+SDM, solid ones with no marks the results by GNASH, and dashed ones LA150 evaluations. Calculation of GNASH and QMD+SDM result to almost similar productions of n , d , and ^3He at the incident energy about 150 MeV. For p , t , α emission, however, serious disagreement between the calculations appear about with a factor of 3.

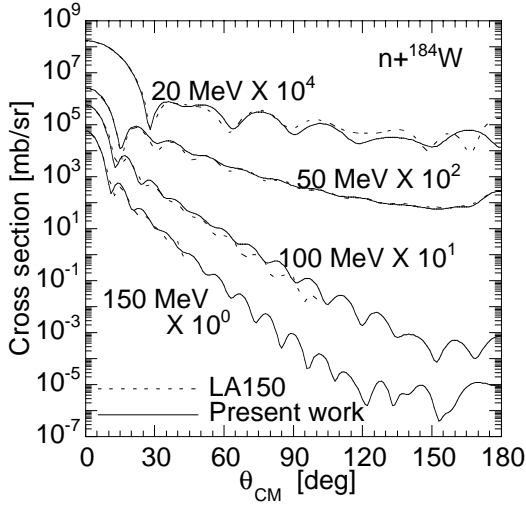


Figure 4: Elastic angular distribution of ^{184}W

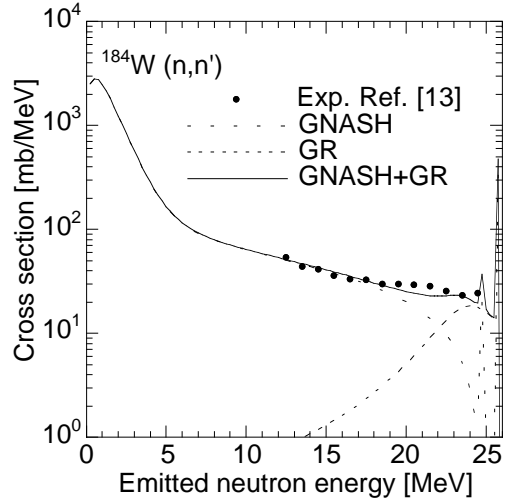


Figure 5: 26MeV neutron-induced neutron production cross section

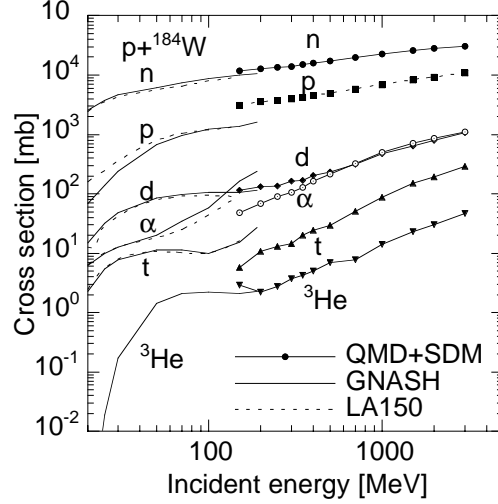
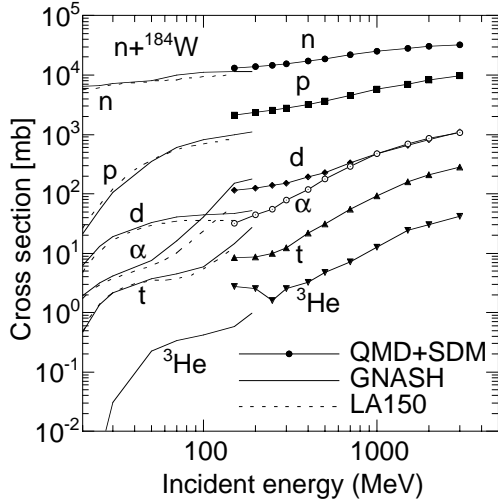


Figure 6: Particle production cross section induced by protons and neutrons up to 3 GeV

3.3 Nucleon emission double differential spectra

Proton incident neutron production double differential cross sections from ^{184}W target are shown in Fig 7. Marks stand for the experimental data[14][15], dashed curves the neutron data computed by QMD+SDM, and solid curves the results analyzed by use of the MS model utilizing the Gaussian-term. The MS model with Gaussian-term reproduced the experimental and calculated neutron data in the whole emission angle region well. Figure 8 shows neutron emission spectra induced by 1 GeV protons and neutrons. Dotted and dashed-dotted curves represent QMD+SDM calculation for (p, xn) and (n, xn) reaction, respectively. Difference of cross section derived from incident nucleon locally appears for emission neutron energies corresponding to the component of cascade process in the MS model. In this study, the common quantities are evaluated for the parameters of the preequilibrium and the evaporation processes to reduce number of MS model parameters.

In Fig. 9, amplitude parameters A_i of the MS model are shown for (p, xn) , (n, xn) , (p, xp) and (n, xp) reactions on ^{184}W target. Marks are the quantities by fitting to individual target mass number and incident nucleon energy. The solid lines are systematics of MS model parameters.

4 Concluding remarks

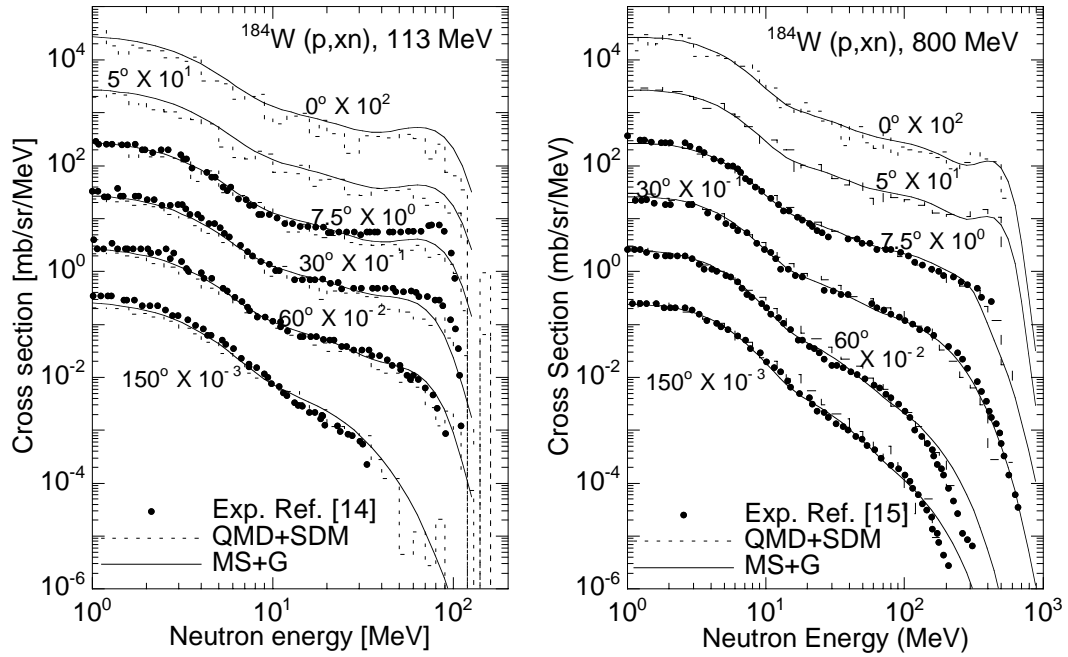


Figure 7: 113 MeV and 800 MeV proton induced neutron production double differential cross section of ^{184}W

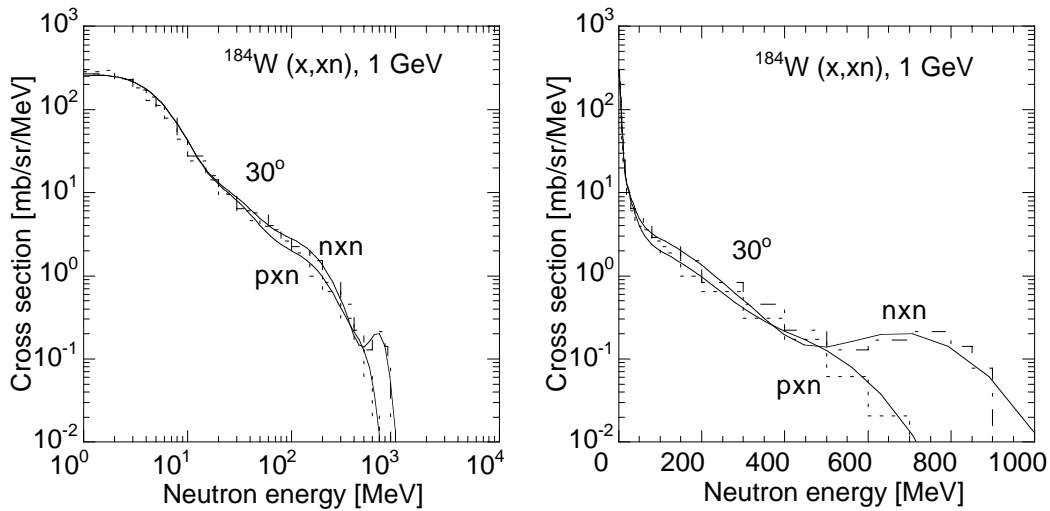


Figure 8: Neutron production double differential cross section of ^{184}W induced by 1 GeV protons and neutrons

New optical potential parameters made by modification of ones by Walter and Guss and by Madland reproduced neutron and proton cross section up to 250 MeV. For light particle production cross sections in the incident energy region about at 170 MeV, large difference of cross sections between calculations of GNASH and QMD+SDM are found. It is seemed that some adjustments of the cross sections in the energy region are required for nuclear data evaluation. Nucleon production double differential cross sections for (p, xn) , (n, xn) , (p, xp) and (n, xp) reactions were evaluated by use of the MS model combining Gaussian term.

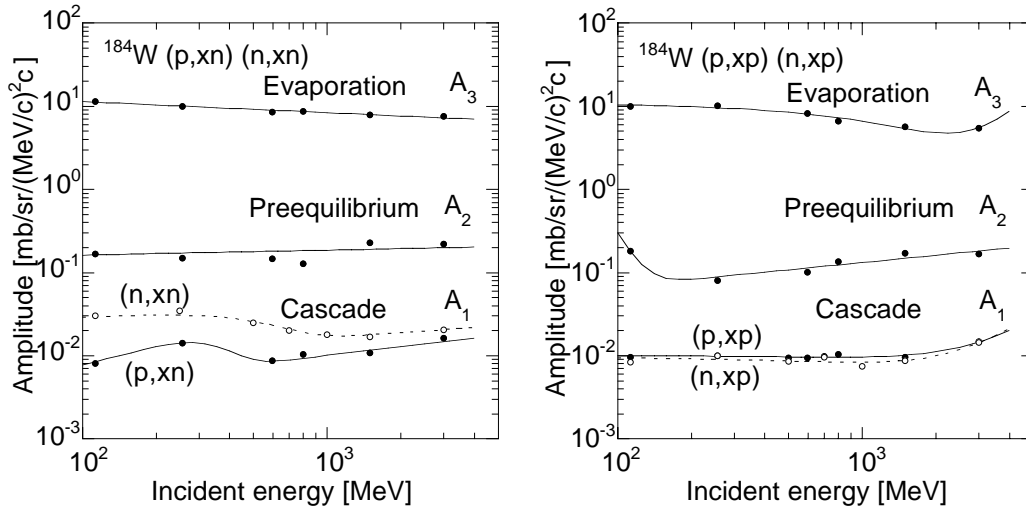


Figure 9: The Amplitude parameter A_i of the MS model

References

- [1] Young, P.G., *et al.* : *Comprehensive Nuclear Model Calculations : Introduction to the Theory and Use of the GNASH Code* ,” LA-22343-MS (1992).
- [2] Niita, K., *et al.* : *Phys. Rev.*, **C52**, 2620 (1995).
- [3] Yamano, T. : *private communication*.
- [4] Kitsuki, H. *et al.* : *J. Nucl. Eng. Soc.*, to be published.
- [5] Marcinkowski, A., Demetriou, P., Hodgson, P.E. : *J. Phys. G.*, **22**, 1219 (1996).
- [6] Walter, R.L., Guss, P.P. : *Rad. Eff.*, **95**, 73 (1986).
- [7] Young, P.G., Madland, D.G. : IAEA INDC(NDS)-335, 109 (1995).
- [8] Dietrich, T.S., *et al.* : *Proc.Int. Conf. Nuclear Data for Science and Technology*, Trieste, Italy, May 19-24, 1997, 402 (1997).
- [9] Hildebrand, R.H., Leith, C.E. : *Phys. Rev.*, **80**, 842 (1950).
- [10] Finlay, R.W., *et al.* : *Phys. Rev.*, **C47**, 237 (1993).
- [11] Kirkby, P., Link, W.T. : *Can. J. Phys.*, **44**, 1847 (1966).
- [12] Abegg, R., *et al.* : *Nucl. Phys.*, **A324**, 109 (1979).
- [13] Marcinkowski, A., *et al.* : *Nucl. Phys.*, **A501**, 1 (1989).
- [14] Amian, W.B. *et al.* : *Nucl. Sci. Eng.*, **102**, 310 (1989).
- [15] Amian, W.B. *et al.* : *Nucl. Sci. Eng.*, **112**, 78 (1992).